ARTICLES
PUBLISHED ONLINE: 13 SEPTEMBER 2009 | DOI: 10.1038/NCHEM.360
nature chemistry

An optoelectronic nose for the detection of toxic gases

Sung H. Lim[1†], Liang Feng[2†], Jonathan W. Kemling[2], Christopher J. Musto[2] and Kenneth S. Suslick[2*]

We have developed a simple colorimetric sensor array that detects a wide range of volatile analytes and then applied it to the detection of toxic gases. The sensor consists of a disposable array of cross-responsive nanoporous pigments with colours that are changed by diverse chemical interactions with analytes. Although no single chemically responsive pigment is specific for any one analyte, the pattern of colour change for the array is a unique molecular fingerprint. Clear differentiation among 19 different toxic industrial chemicals (TICs) within two minutes of exposure at concentrations immediately dangerous to life or health were demonstrated. Based on the colour change of the array, quantification of each analyte was accomplished easily, and excellent detection limits were achieved, generally below the permissible exposure limits. Different TICs were identified readily using a standard chemometric approach (hierarchical clustering analysis), with no misclassifications over 140 trials.

There is an obvious pressing need for the rapid, sensitive and highly portable identification of toxic gases and vapours, not only from a security perspective, but also for use in the industrial chemical workplace and for more general epidemiological studies[1]. Almost by definition, toxic industrial chemicals (TICs) are chemically reactive. Their toxicities, however, derive from a very wide range of specific chemical reactivities that can affect vastly different systems within living organisms. Some acute toxins target specific, critical metabolic enzymes (for example, hydrogen cyanide inhibits cytochrome c oxidase), and others cause cell lysis in the lungs and so create pulmonary oedema (for example, hydrogen chloride and hydrogen fluoride). Some are potent oxidants or reductants that can target multiple biosystems, and others are potent alkylating agents (for example, phosgene).

We approached the detection and identification of TICs by presenting a wide range of chemical substrates that reacted with these analytes to provide an easily observable response, specifically colour changes quantified by digital imaging. Such an 'optoelectronic nose' is array-based chemical sensing founded on the biomimetic concept of using many cross-responsive sensor elements[2–5], rather than analyte-specific lock-and-key receptors. As with the mammalian olfactory system[6–8], it is the composite response of the chemical reactivity of such an array that identifies an odorant or mixture of odorants. Our optoelectronic nose uses a colorimetric sensor array (CSA) that largely overcomes the limitations of prior electronic nose technologies, and we report here its use for the identification of a wide range of TICs at low concentrations.

In contrast to our chemical reactivity approach, other electronic nose technologies[9–18] generally rely on sensors with responses that originate from weak and highly non-specific chemical interactions that either induce changes in physical properties (for example, mass, volume or conductivity) or occur after physisorption on surfaces (for example, analyte oxidation on heated metal oxides). Specific examples of such sensors include conductive polymers and polymer composites, multiple polymers doped with a single fluorescent dye, polymer-coated surface acoustic wave devices and metal-oxide sensors. As a consequence of this reliance on weak interactions, most electronic nose technologies suffer from severe limitations: the detection of compounds at low concentrations relative to their vapour pressures is difficult, the discrimination between compounds within a similar chemical class is limited and, importantly, interference from environmental changes in humidity remains problematic.

The design of our CSA[2–5,19–26] is based on stronger dye–analyte interactions than those that cause simple physical adsorption; the array incorporates a diverse set of chemically responsive colourants, including metalloporphyrins and various families of dyes. More specifically, we have chosen chemically responsive dyes in four classes (Fig. 1): (1) dyes containing metal ions (for example, metalloporphyrins) that respond to Lewis basicity (that is, electron-pair donation, metal-ion ligation), (2) pH indicators that respond to Brønsted acidity and basicity (that is, proton acidity and hydrogen bonding), (3) dyes with large permanent dipoles (for example, vapochromic or solvatochromic dyes) that respond to local polarity and (4) metal salts that respond to redox reactions. The importance of including sensors that contain metal ions in such an array is confirmed by indications that the mammalian olfactory receptors are likely to be metalloproteins[7,8].

In recent related work, we reported[24–26] a new array methodology specific to liquid sensing that is based on nanoporous pigments created by the immobilization of pH indicators in organically modified siloxanes (ormosils[27]). Nanoporous pigments offer substantial advantages over soluble dyes because they improve durability and stability of the array, and also prevent colourant leaching in aqueous media. Here, we report an extension of these new nanoporous pigment arrays using a much broader range of chemically responsive pigments. We applied these arrays to identify TICs in the gas phase colorimetrically and demonstrated substantial improvements in the array sensitivity at low gas concentrations.

Results and discussion

The chemically responsive indicators used in CSAs have been limited to soluble molecular dyes held in a semifluid polymer film and generally printed onto a porous membrane[2–5,19–23]. Relative to insoluble pigments, chemically responsive dyes in the semifluid state are often unstable over long periods of storage. Non-porous

[1]iSense LLC, 470 Ramona St, Palo Alto, California 94301, USA, [2]Department of Chemistry, University of Illinois at Urbana-Champaign, 600 South Mathews Avenue, Urbana, Illinois 61801, USA; [†]Both authors contributed equally to this work. *e-mail: ksuslick@illinois.edu

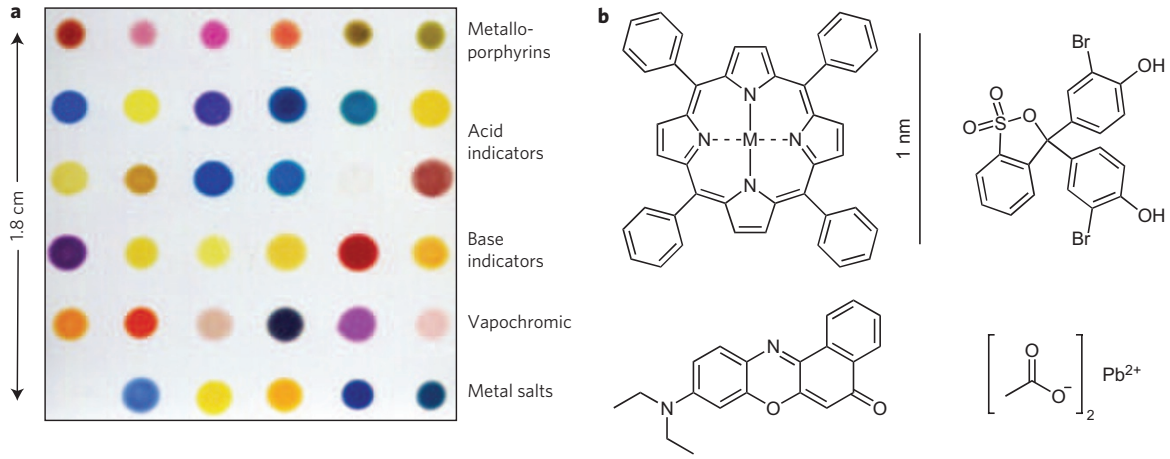

Figure 1 | The CSA consists of 36 different chemically responsive pigments printed directly on a polyethylene terephthalate film. a, An image of the array from an ordinary flatbed scanner with the different pigment classes labelled. **b**, Molecular structures of examples from each dye class; to absorb visible light, dyes are inherently of nanometre scale. The 36 dyes were selected empirically based on the quality of their colour response to a representative selection of chemically diverse analytes.

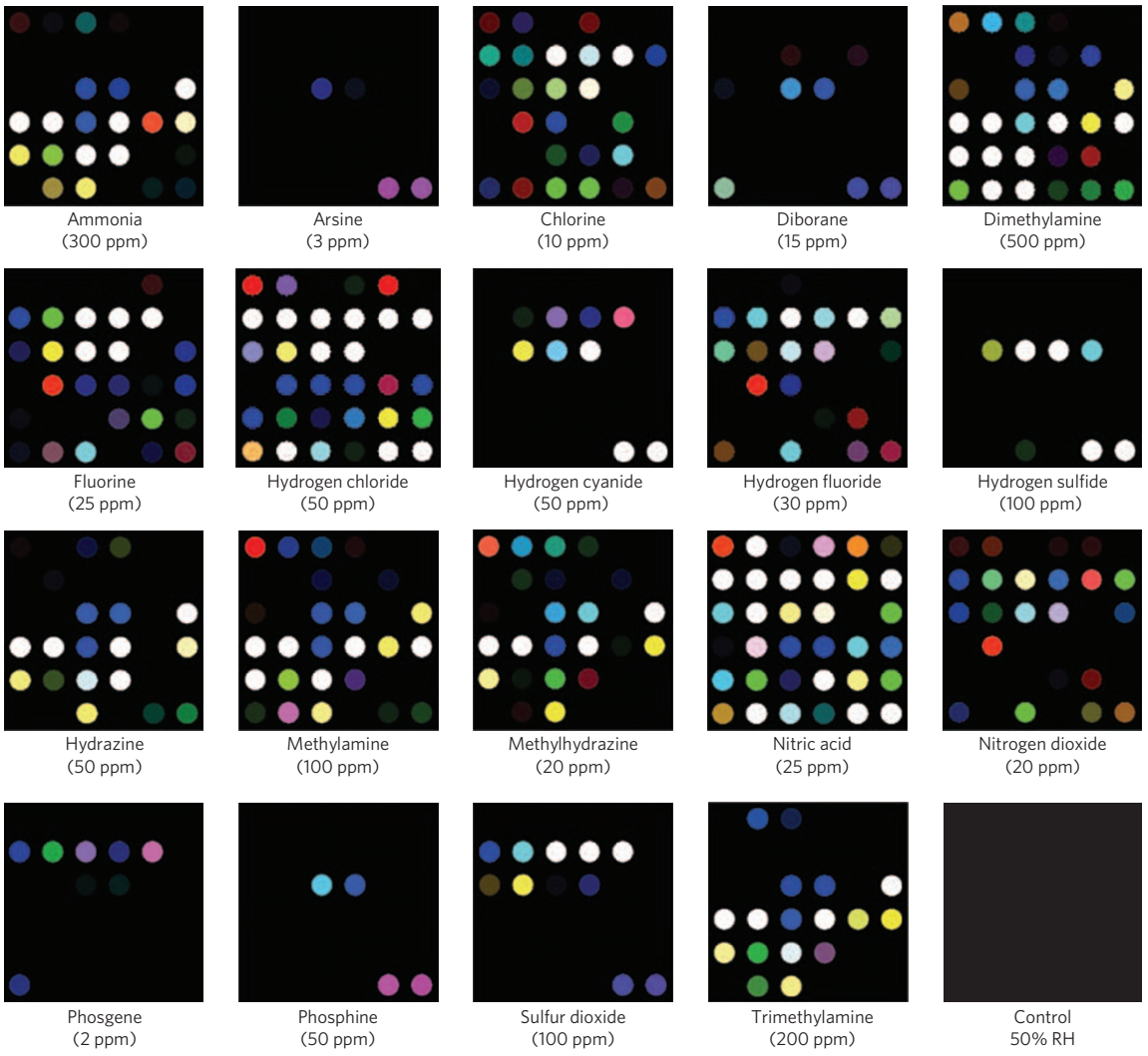

Figure 2 | Colour-change profiles of representative TICs at their IDLH concentration after two minutes of exposure. The IDLH concentrations are listed under each analyte in parts per million (ppm). A full digital database is provided in Supplementary Table S3. For display purposes, the colour ranges of these difference maps are expanded from four to eight bits per colour (red, green and blue range of 4–19 expanded to 0–255). RH = relative humidity.

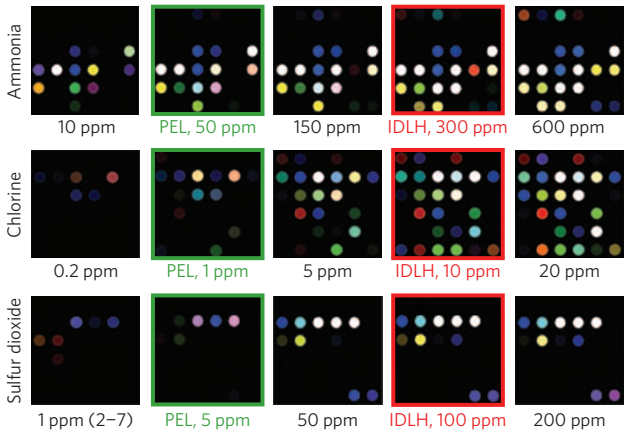

Figure 3 | The effect of concentration on array response to ammonia, chlorine and sulfur dioxide. The colour-change profiles of these three representative TICs are shown over roughly a 100-fold range of concentration. The observed LODs are well below the PEL. For display purposes, the colour ranges of these difference maps are expanded from four to eight bits per colour (red, green and blue range of 4–19 expanded to 0–255), except for that of sulfur dioxide at 1 ppm (red, green and blue range of 2–7 expanded to 0–255).

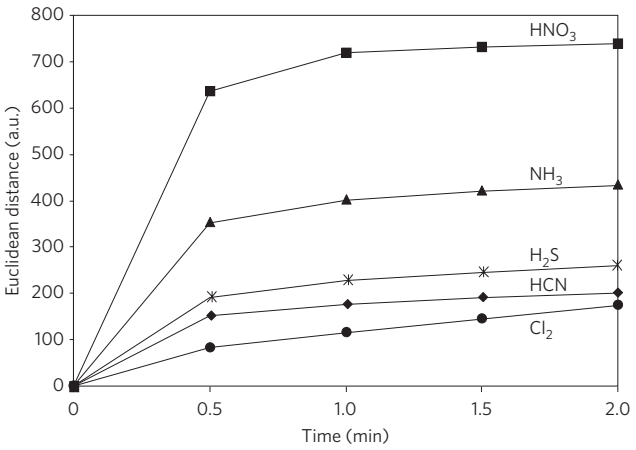

Figure 4 | Response time of the array. Total Euclidean distance of the array plotted versus time for five representative TICs at their IDLH concentrations; the average of seven trials is shown. The Euclidean distance is simply the total length of the 108-dimensional colour-difference vector, that is, the total array response.

pigments, however, generally do not provide sufficient contact between the analyte and the chromophores of the pigment, because the chromophores at the surface of the pigment are usually only a small fraction of the total number of chromophores.

There is, though, a general method to incorporate chemically responsive dyes into porous matrices, and thus create nanoporous pigments that can provide both stability and analyte access to the chromophores. Among various host materials, ormosils provide excellent matrices for a variety of organic and inorganic colourants[27–30]. Furthermore, the final properties of the nanoporous pigments (for example, hydrophobicity, porosity and surface area) can be modified easily by controlling the physical and chemical parameters of the sol–gel process. To print our sensor arrays, we prepared solutions of sol–gel colourant by the simple hydrolysis of solutions that contained commercially available silane precursors (for example, tetraethoxysilane, methyltriethoxysilane, phenethyltrimethoxysilane and octyltriethoxysilane) with a variety of chemically responsive indicators.

This conversion of soluble dyes into nanoporous ormosil pigments significantly improves stability[27–30]. We found that there is no change in the analyte response for arrays stored for at least three months[26]. Importantly, our sol–gel formulation permits simple printing onto ordinary flat surfaces of polymer, which allowed an easy packaging of the sensor array into a self-sealing cartridge with minimal dead space (Supplementary Fig. S1) suitable for use with a handheld battery-operated scanner (Supplementary Fig. S2). In addition, we found that the porous matrix improved the sensitivity of the sensor. Compared with previous results with highly plasticized dye sensor arrays, we found an improvement in sensitivity of ~800% at low concentrations. Our hypothesis is that the nanoporous matrix may serve as an *in situ* preconcentrator for analytes.

As an important application of this new optoelectronic nose, we began an examination of TICs, choosing 19 representative examples from lists generated by International Task Force 25 and 40 reports[31,32]. The immediately dangerous to life or health (IDLH) concentrations of these TICs are given in Supplementary Table S2. Detection and discrimination among the wide range of high-priority TICs remains a major challenge[33] and the subject of substantial recent research. For example, recently Hammond *et al.* reported on TIC identification using an array of ceramic metallic films; they were able to differentiate ten TICs with an error rate of ~10% using a linear discriminant analysis[34]. Using metal-oxide

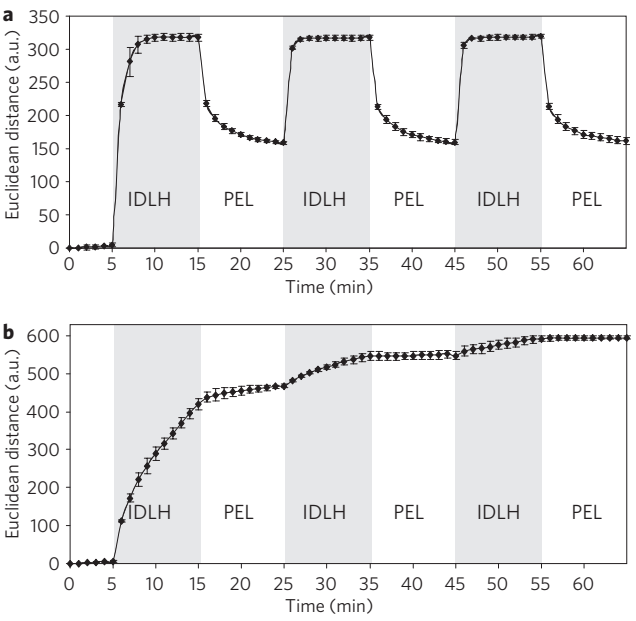

Figure 5 | Reversibility of colorimetric array response. a, Sulfur dioxide exposure of the array from nitrogen to the IDLH (100 ppm) level, and then repeatedly from the IDLH to PEL (5 ppm) and back. **b**, Chlorine exposure of the array from nitrogen to the IDLH (10 ppm) level, and then repeatedly from the IDLH to PEL (1 ppm) and back. Data were acquired every minute. The response times in these data reflect the dead volume in the gas-mixing system and do not represent the intrinsic response of the array (which is shown in Fig. 4). The error bars shown are the standard deviation of triplicate trials.

detectors combined with temperature programming, Meier *et al.*[35] examined five TICs and were able to reduce their error rate (both false negatives and positives) to 3%.

We tested our CSA extensively against 19 TICs at their IDLH concentrations at 50% relative humidity. The CSAs were exposed for two minutes to a diluted gas mixture produced either from premixed, certified gas cylinders or from saturated vapour, using digital mass-flow controllers (configurations are shown in Supplementary Fig. S3). Importantly, gas-stream concentrations were confirmed using

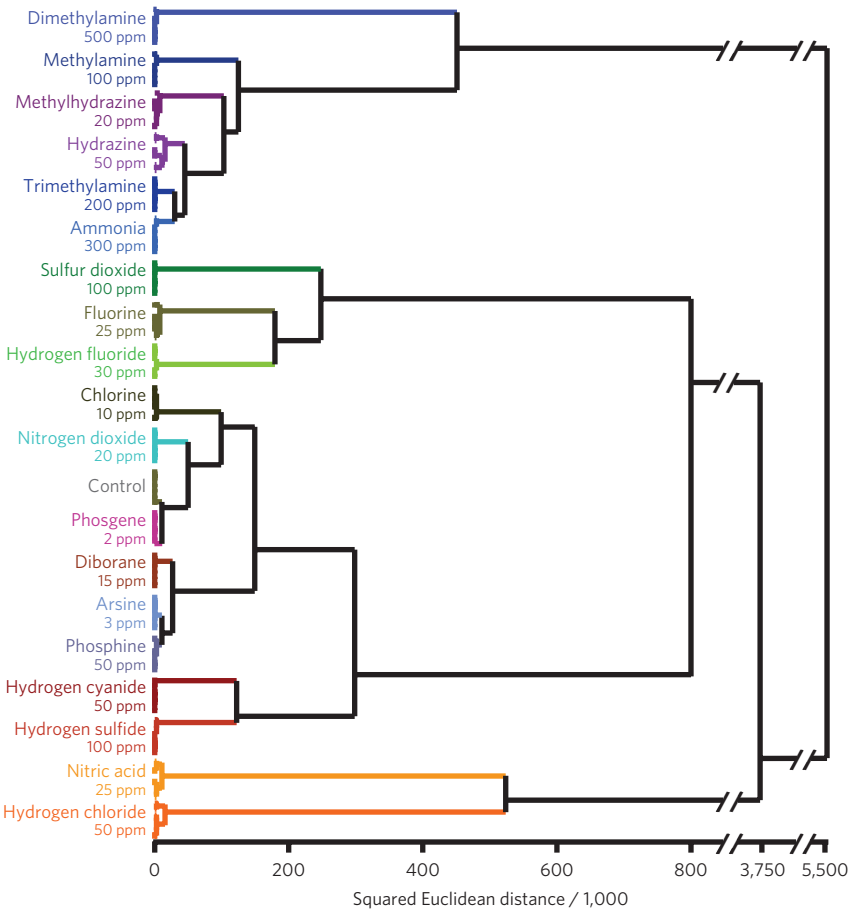

Figure 6 | HCA for 19 TICs at IDLH concentrations and a control. HCA is a routine model-free statistical classification method based on Euclidean distance[36–39]. In these experiments, the Euclidean distances are defined by the colour-difference vectors of each experimental trial in the full 108-dimensional space made up of the changes in red, green and blue values of the 36 nanoporous pigments in the sensor array. As shown, all experiments were run in septuplicate: no confusions or errors in classification were observed in 140 trials. The HCA used minimum variance (that is, 'Ward's Method') for clustering.

in-line analysis by Fourier transform infrared spectroscopy (FTIR) in real time with a MKS multigas analyser for most analytes, or by Dräger detector tubes for the few cases in which FTIR could not be used (for example, the homonuclear diatomics chlorine and fluorine).

The printed arrays were imaged digitally with an ordinary flatbed scanner before and after exposure to each analyte. Colour-difference maps for the arrays were generated by subtraction of the image before exposure from that after exposure: such difference maps provide molecular fingerprints that effectively identify the analyte to which the array has been exposed. The difference maps permit facile detection and identification of the 19 representative TICs, as shown in Fig. 2. Even by eye, without statistical analysis, the array response to each TIC is represented by a unique pattern. For quantitative analysis of the difference maps, we can define a 108-dimensional vector (that is, 36 changes in red, green and blue values for the after-exposure image compared with the before-exposure image for our 6×6 array of nanoporous pigments). In this fashion, it is not necessary to retain the full digital images: each analyte is represented digitally by the 108-dimensional vector and may be compared by standard chemometric techniques. Simple comparisons of the Euclidean distance between an observed colour difference vector and a precollected library are extremely rapid (subsecond); even a large library requires only minimal memory (for example, 1,000 entries need 148 kB zip-compressed). The raw, digital colour-difference vectors from a total of 140 experimental trials are given in Supplementary Tables S3 and S4.

For most analytes, the response of these CSAs is based primarily on equilibrium interactions between the array pigments and the analyte, and consequently each concentration of a TIC has a separate pattern that can be used to establish a limit of detection (LOD). As examples, colour-change profiles for three different analytes as a function of concentration are given in Fig. 3. Here, the LODs for all three examples are well below their respective permissible exposure limits (PELs). Although highly dependent on the analyte, our estimates for the LODs of the TICs examined are all well below their respective PELs.

Most of the TICs can be identified from the array colour change in a matter of seconds, and $>90\%$ of total response is observed in less than two minutes, as shown in Fig. 4 for five representative TICs; all the other TICs tested show very similar responses. For some aggressive analytes that undergo irreversible reactions with some pigments (for example, bleaching), response time can be slightly longer, as for chlorine (Fig. 4), but even in these cases the colour-change pattern is distinctive and easily recognized.

Although the CSAs are meant to be disposable, they are still reusable for most analytes. The CSA is best thought of as a 'chemical fuse': just as with an electric fuse, as long as the concentration of the odorant (that is, 'the electric current') fluctuates within some range, the CSA ('fuse') is unaffected. However, if the concentration increases to too high a value, the CSA takes too long to recover; that is, the fuse is blown and the CSA should be replaced. As illustrated in Fig. 5a, the CSA reproducibly cycles between the IDLH and PEL concentrations of many of the TICs (sulfur dioxide, for example). After switching from one concentration to the other, equilibrium response is achieved within two minutes. The reversibility of the array is dependent on the type of chemical

interaction between the pigments and the analytes, and for irreversible reactions with highly aggressive analytes (for example, those capable of bleaching or redox reactions), the array cannot be recycled, as demonstrated in Fig. 5b for chlorine. For other gases, notably arsine and phosphine, the reduction of metal salts that generates metal nanoparticles produces the acidic by-products that are detected by pH indicators incorporated into the nanoporous sol–gel spot. Finally, the response to phosgene is caused by an alkylation reaction with 4-(4-nitrobenzyl)pyridine within the sol–gel matrix.

In practical situations in the field, control over the humidity is unlikely, which can be extremely problematic for other electronic nose technologies. We selected hydrophobic colourants and sol–gel matrices so that changes in humidity would present no difficulty. As shown in Supplementary Fig. S4, the colour-difference maps are unaffected by changes in relative humidity from 10% to 90%.

The colour-change profiles are inherently digital data and easily handled by routine chemometric analysis[36–39]. The high dispersion of the data array of the colorimetric sensor requires a classification algorithm that uses the full dimensionality of the data. The simplest statistical approach is hierarchical cluster analysis (HCA), which is a classification scheme based on the Euclidean distance between data points in their full dimensionality. The advantage of HCA compared with other model-dependent statistical analyses (for example, linear discriminant analysis) is that it makes no assumptions about the classification of results one is trying to establish. Each experimental trial is defined as a 108-dimensional vector that consists of the changes in red, green and blue values of each of the 36 nanoporous pigments in our array. Hierarchical clustering is based on the Euclidean distance in this 108-dimensional red, green and blue colour space among these vectors, which generates a dendrogram, as shown in Fig. 6. Remarkably, in septuplicate trials, all 19 TICs and a control were identified accurately against one another with no errors or misclassifications out of 140 cases.

The ability of our CSAs to discriminate so many analytes from one another is impressive and largely the result of the extremely high dimensionality of the array data. Principal component analysis can be used to determine the number of meaningful independent dimensions probed by a cross-reactive array. The eigenvector of each principal component defines the linear combination of the response of each sensor parameter by the amount of variance in the data along each principal component. Based on the 140 trials on 20 analytes (that is, 19 TICs plus background), the principal component analysis of our CSA requires nine dimensions for 90% total variance (and 13 dimensions for 95%, as shown in Supplementary Fig. S5). This extremely high dispersion reflects the very wide range of chemical properties space probed by our choice of chemoresponsive pigments. As a consequence, chemically diverse analytes are recognized easily, and even closely related mixtures can be distinguished[2–4]. In contrast, data from most electronic nose technologies are dominated by only two or three independent dimensions (one of which, analyte hydrophobicity, generally accounts for >90% of total variance); this is the inherent result of relying on van der Waals and other weak interactions (for example, adsorption to metal-oxide surfaces or absorption onto or into polymer films) for molecular recognition.

Conclusions

In summary, we have created a simple, disposable CSA of nanoporous pigments that is able to detect a wide range of analytes. By immobilizing chemically responsive indicators within nanoporous sol–gel matrices, we can apply the sensor array to the detection of volatile TICs and observe low detection limits, generally below the PELs. Classification analysis reveals that the CSA has an extremely high dimensionality and, consequently, the ability to discriminate among large numbers of TICs over a wide range of concentrations.

Although the laboratory studies reported here made use of inexpensive flatbed scanners for imaging, we recently constructed a fully functional prototype handheld device that makes use of an inexpensive white LED (light-emitting diode) and an ordinary CMOS (complementary metal-oxide semiconductor) camera, as shown in Supplementary Fig. S2; indeed, the signal-to-noise ratios of the images taken with this prototype are a factor of three better than those of our flatbed scanners. Combined with a low dead-volume cartridge (Supplementary Fig. S1), this handheld device is a rapid, inexpensive and highly sensitive method for the portable monitoring of ambient toxic gases. Further development, we expect, will lead to a wearable device: that is, the chemist's equivalent of a physicist's radiation badge.

Methods

Reagents. All the reagents were of analytical grade obtained from Sigma-Aldrich and used without any further purification unless otherwise specified. Certified, premixed gas tanks, including ammonia, methylamine, dimethylamine, trimethylamine, hydrogen chloride, sulfur dioxide, fluorine, chlorine, phosphine, arsine, phosgene, hydrogen sulfide, hydrogen cyanide and diborane were obtained from Matheson Tri-Gas through S. J. Smith.

Array printing. The colourant indicators are given in Supplementary Table S1. Final organically modified sol–gel (ormosil) formulations and the colourants were loaded into a 36-hole Teflon inkwell. Sensor arrays were printed using an array of 36 floating slotted pins (which delivered approximately 130 nl each) by dipping into the inkwell and transferring to the polyethylene terephthalate film. Once printed, the arrays were aged under nitrogen for at least three days before any sensing experiment was performed.

Experimental procedure. The TICs at their IDLH concentrations (see Supplementary Table S2) were prepared by mixing the gas stream of prediluted analyte with dry and wet nitrogen gas using MKS digital mass-flow controllers to achieve the desired concentrations and relative humidity (see Supplementary Fig. S2). For nitric acid and hydrogen fluoride, saturated vapours were generated from a diluted solution in a five-gallon polyethylene carboy, which was further diluted to the IDLH concentration with nitrogen gas. Hydrazine (98%) was used directly to produce saturated hydrazine vapour. Importantly, gas-stream concentrations and relative humidity were confirmed by in-line analysis with FTIR using a MKS multigas analyser, model 2030. In our experience, the independent in-line analysis of tank gases is absolutely essential, even with the manufacturer's certification; premixed tanks of these reactive gases at the low concentrations used here (typically four times the IDLH) do not necessarily retain their original certified concentrations. Fluorine, chlorine, hydrazine, nitric acid and hydrogen fluoride at their IDLH concentrations were confirmed using Dräger detector tubes.

Data analysis. For all sensing experiments, imaging of the arrays was done on an ordinary flatbed scanner (Epson Perfection V200); for good reproducibility, it is important to 'warm-up' the scanner. Difference maps were obtained by taking the difference of the red, green and blue values from the centre of every colourant spot (~300 pixels) from the 'before' and 'after' images. To eliminate the possibility of subtraction artefacts caused by variations in colour near the spot edge, only the spot centre was included in the calculation. Averaging of the centres of the spots avoids artefacts caused by non-uniformity of the printing of the spots, especially at their edges. Subtraction of the two images yields a colour-difference vector of $3N$ dimensions, where $N =$ the total number of spots. For our 6×6 array, this difference vector is 108 dimensions (that is, 36 changes in red, green and blue colour values), with each dimension ranging from -255 to $+255$ for eight-bit colour imaging. The difference vectors are provided in Supplementary Tables S3 and S4. Measurements can be performed using Adobe Photoshop or with a customized software package, ChemEye (ChemSensing). All experiments were run in septuplicate, and chemometric analyses were carried out on the difference vectors using the Multi-Variate Statistical Package (v. 3.1, Kovach Computing).

Humidity experiments. Relative humidity was controlled by mixing dry nitrogen with humidity-saturated nitrogen (100% relative humidity, generated by bubbling nitrogen through water). Using 50% relative humidity as a control, arrays were exposed to various humidity concentrations for two minutes (see Supplementary Fig. S4); no significant response to humidity was observed from 10% to 90% relative humidity.

Cycling experiments. Sulfur dioxide and chlorine gases at PEL concentrations were prepared using the same method as for IDLH concentrations. The CSA was exposed to nitrogen (50% relative humidity) for five minutes, and then the gas stream switched from IDLH to PEL and back every ten minutes. Data was acquired every minute.

Received 26 June 2009; accepted 5 August 2009; published online 13 September 2009

References

1. Byrnes, M. E., King, D. A. & Tierno, P. M. Jr *Nuclear, Chemical, and Biological Terrorism – Emergency Response and Public Protection* (CRC Press, 2003).
2. Suslick, K. S. *et al.* Seeing smells: development of an optoelectronic nose. *Quimica Nova* **30,** 677–681 (2007).
3. Suslick, K. S. An optoelectronic nose: seeing smells by means of colorimetric sensor arrays. *MRS Bull.* **29,** 720–725 (2004).
4. Suslick, K. S., Rakow, N. A. & Sen, A. Colorimetric sensor arrays for molecular recognition. *Tetrahedron* **60,** 11133–11138 (2004).
5. Rakow, N. A. & Suslick, K. S. A colorimetric sensor array for odour visualization. *Nature* **406,** 710–713 (2000).
6. Hawkes, C. H. & Doty, R. L. *The Neurology of Olfaction* (Cambridge Univ. Press, 2009).
7. Zarzo, M. The sense of smell: molecular basis of odorant recognition. *Biol. Rev.* **82,** 455–479 (2007).
8. Wang, J., Luthey-Schulten, Z. A. & Suslick, K. S. Is the olfactory receptor a metalloprotein? *Proc. Natl Acad. Sci. USA* **100,** 3035–3039 (2003).
9. Gardner, J. W. & Bartlett, P. N. *Electronic Noses: Principles and Applications* (Oxford Univ. Press, 1999).
10. Lewis, N. S. Comparisons between mammalian and artificial olfaction based on arrays of carbon black–polymer composite vapor detectors. *Acc. Chem. Res.* **37,** 663–672 (2004).
11. Röck, F., Barsan, N. & Weimar, U. Electronic nose: current status and future trends. *Chem. Rev.* **108,** 705–725 (2008).
12. Hierlemann, A. & Gutierrez-Osuna, R. Higher-order chemical sensing. *Chem. Rev.* **108,** 563–613 (2008).
13. Anslyn, E. V. Supramolecular analytical chemistry. *J. Org. Chem.* **72,** 687–699 (2007).
14. Walt, D. R. Electronic noses: wake up and smell the coffee. *Anal. Chem.* **77,** 45A (2005).
15. Wolfbeis, O. S. Materials for fluorescence-based optical chemical sensors. *J. Mater. Chem.* **15,** 2657–2669 (2005).
16. Hsieh, M.-D. & Zellers, E. T. Limits of recognition for simple vapor mixtures determined with a microsensor array. *Anal. Chem.* **76,** 1885–1895 (2004).
17. Janata, J. & Josowicz, M. Conducting polymers in electronic chemical sensors. *Nature Mater.* **2,** 19–24 (2003).
18. Grate, J. W. Acoustic wave microsensor arrays for vapor sensing. *Chem. Rev.* **100,** 2627–2647 (2000).
19. Rakow, N. A., Sen, A., Janzen, M. C., Ponder, J. B. & Suslick, K. S. Molecular recognition and discrimination of amines with a colorimetric array. *Angew. Chem. Int. Ed.* **44,** 4528–4532 (2005).
20. Janzen, M. C., Ponder, J. B., Bailey, D. P., Ingison, C. K. & Suslick, K. S. Colorimetric sensor arrays for volatile organic compounds. *Anal. Chem.* **78,** 3591–3600 (2006).
21. Zhang, C. & Suslick, K. S. A colorimetric sensor array for organics in water. *J. Am. Chem. Soc.* **127,** 11548–11549 (2005).
22. Zhang, C., Bailey, D. P. & Suslick, K. S. Colorimetric sensor arrays for the analysis of beers: a feasibility study. *J. Agric. Food Chem.* **54,** 4925–4931 (2006).
23. Zhang, C. & Suslick, K. S. Colorimetric sensor array for soft drink analysis. *J. Agric. Food Chem.* **55,** 237–242 (2007).
24. Lim, S. H., Musto, C. J., Park, E., Zhong, W. & Suslick, K. S. A colorimetric sensor array for detection and identification of sugars. *Org. Lett.* **10,** 4405–4408 (2008).
25. Bang, J. H., Lim, S. H., Park, E. & Suslick, K. S. Chemically responsive nanoporous pigments: colorimetric sensor arrays and the identification of alipathic amines. *Langmuir* **24,** 13168–13172 (2008).
26. Musto, C. J., Lim, S. H. & Suslick, K. S. Colorimetric detection and identification of natural and artificial sweeteners. *Anal. Chem.* **81,** 6526–6533 (2009).
27. Podbielsk, H., Ulatowska-Jarza, A., Muller, G. & Eichler, H. J. *Optical Chemical Sensors* (Springer, 2006).
28. Dunbar, R. A., Jordan, J. D. & Bright, F. V. Development of chemical sensing platforms based on sol–gel-derived thin films: origin of film age vs. performance trade-offs. *Anal. Chem.* **68,** 604–610 (1996).
29. Jeronimo, P. C. A., Araujo, A. N. & Montenegro, M. Optical sensors and biosensors based on sol–gel films. *Talanta* **72,** 13–27 (2007).
30. Rottman, C., Grader, G., De Hazan, Y., Melchior, S. & Avnir, D. Surfactant-induced modification of dopants reactivity in sol–gel matrixes. *J. Am. Chem. Soc.* **121,** 8533–8543 (1999).
31. Steumpfle, A. K., Howells, D. J., Armour, S. J. & Boulet, C. A. *Final Report of International Task Force 25: Hazard From Toxic Industrial Chemicals* (US GPO, Washington, DC) http://file.sunshinepress.org:54445/us-uk-ca-mou-itf25-1996.pdf (1996).
32. Armour, S. J. *et al. International Task Force 40: Toxic Industrial Chemicals (TICs)—Operational and Medical Concerns* (US GPO, Washington, DC) <http://chppm-www.apgea.army.mil/desp/pages/jeswg/4QFY01/itf-40-2US.ppt> (2001).
33. Hill, H. H. & Martin, S. J. Conventional analytical methods for chemical warfare agents. *Pure Appl. Chem.* **74,** 2281–2291 (2002).
34. Hammond, M. H. *et al.* A novel chemical detector using cermet sensors and pattern recognition methods for toxic industrial chemicals. *Sens. Actuat. B* **116,** 135–144 (2006).
35. Meier, D. C. *et al.* The potential for and challenges of detecting chemical hazards with temperature-programmed microsensors. *Sens. Actuat. B* **121,** 282–294 (2007).
36. Hasswell, S. *Practical Guide To Chemometrics* (Dekker, 1992).
37. Scott, S. M., James, D. & Ali, Z. Data analysis for electronic nose systems. *Microchim. Acta* **156,** 183–207 (2007).
38. Johnson, R. A. & Wichern, D. W. *Applied Multivariate Statistical Analysis* 6th edn (Prentice Hall, 2007).
39. Hair, J. F., Black, B., Babin, B., Anderson, R. E. & Tatham, R. L. *Multivariate Data Analysis* 6th edn (Prentice Hall, 2005).

Acknowledgements

This work was supported through the National Institutes of Health Genes, Environment and Health Initiative through award U01ES016011.

Author contributions

S.H.L. and L.F. contributed equally to the design of experiments, collection and analysis of data, and drafting of the manuscript, with assistance from J.W.K. and C.J.M. K.S.S. originated the central idea, oversaw the design of experiments and data analysis and contributed to the writing of the manuscript.

Additional information

Supplementary information accompanies this paper at www.nature.com/naturechemistry. The authors declare competing financial interests: details accompany the full-text HTML version of the paper at www.nature.com/naturechemistry. Reprints and permission information is available online at http://npg.nature.com/reprintsandpermissions/. Correspondence and requests for materials should be addressed to K.S.S.